Polyhedron 29 (2010) 3229–3237

Contents lists available at ScienceDirect

Polyhedron

journal homepage: www.elsevier.com/locate/poly

Unsymmetrical zinc azaphthalocyanines, peripherally substituted with thiophen-2-yl and 2-functionalized phenoxy groups

Eva H. Mørkved [a,*], Trygve Andreassen [b], Roland Fröhlich [c], Frode Mo [d], Per Bruheim [b]

[a] Norwegian University of Science and Technology, Department of Chemistry, N-7491 Trondheim, Norway
[b] Norwegian University of Science and Technology, Department of Biotechnology, N-7491 Trondheim, Norway
[c] Organisch-Chemisches Institut, Universität Münster, Corrensstrasse 40, D-48149 Münster, Germany
[d] Norwegian University of Science and Technology, Department of Physics, N-7491 Trondheim, Norway

ARTICLE INFO

Article history:
Received 20 July 2010
Accepted 30 August 2010
Available online 1 October 2010

Keywords:
Zinc azaphthalocyanine
Tetrapyrazinoporphyrazine
Thiophen-2-yl
Phenoxy
Pyrazine-2,3-dicarbonitrile
Crystallography
Dichlorobis(quinoline-*N*)zinc(II)

ABSTRACT

Four targeted octasubstituted zinc azaphthalocyanines (ZnAzaPc), substituted with thiophen-2-yl groups and ortho-substituted phenoxy groups, were obtained by cyclotetramerization of 5-aryloxy-6-(thiophen-2-yl)pyrazine-2,3-dicarbonitriles. Thiophen-2-yl substituents are known to extend the macrocyclic conjugation, and thereby cause red-shifted UV–Vis Q-bands. Peripheral phenoxy groups with bulky ortho substituents are expected to suppress aggregation and thereby improve solubility of these compounds. The reagent $Zn(quinoline)_2Cl_2$ was used for one-step syntheses of these ZnAzaPc. Four tetrasubstituted ZnAzaPc, with phenoxy, (2-isopropyloxy)phenoxy, (2-isopropyl)phenoxy or (2-*tert*-butyl)phenoxy substituents, were obtained as controls from 5-aryloxypyrazine-2,3-dicarbonitriles. The tetra- and octa-substituted ZnAzaPc, **5** and **6**, were obtained in 30–50% yields after purification by chromatography on silica. UV–Vis Q-bands with high molar extinction coefficients (100 000–160 000), were observed at 635 nm for compounds **5**, and at 660–665 nm for **6**. Grass-green solutions were obtained of compounds **6** in most organic solvents, whereas the less soluble compounds **5** gave blue-green solutions. 2D NMR methods were applied in analyses of DMSO-d_6 solutions of ZnAzaPc **5** and **6**. Broad and partly overlapping ^{1}H NMR signals for some of the compounds indicate some aggregation as well as presence of two or more structural isomers. Molecular ions of ZnAzaPc **5** and **6** were determined by mass spectrometry (MALDI-TOF).

Structure analyses of 5-phenoxy-6-(thiophen-2-yl)pyrazine-2,3-dicarbonitrile (**4a**), and 5-(2-isopropyloxyphenoxy)-6-(thiophen-2-yl)pyrazine-2,3-dicarbonitrile (**4b**), show the impact on conformation exerted by the bulky isopropyloxy ortho-substituent of the phenoxy group in **4b**, and indicates how this substituent hinders the type of disorder found in **4a**.

1. Introduction

Phthalocyanines (Pc), have served as important industrial blue-green colourants for about 100 years, and during the last two decades both properties and numerous sophisticated applications have been explored for this class of compounds [1]. Tetrapyrazinoporphyrazines, here named azaphthalocyanines (AzaPc), are in general considered less important than the parent phthalocyanines due to different physical properties such as inferior stability, colour, and less resistance to oxidation. However, interest in this class of compounds is steadily increasing, and many applications in materials science have been reported recently [2]. Eight additional nitrogen atoms on the periphery of AzaPc increase the polarity of these macrocycles, and substituents may be used for tuning solubility, UV–Vis absorptions i.e. shifts of Q-bands, and acid–base properties. There is limited knowledge concerning the influence of heteroatom substituents on both synthesis and properties of AzaPc. Several years ago we synthesized some heteroatom substituted AzaPc [3,4] and found that sulfanyl-, and in particular oxo-substituents, of pyrazine-dicarbonitriles could be replaced by nucleophiles during cyclotetramerizations if metal alkoxides and alcohols were used. Similar, but less pronounced problems have been found for cyclizations of sulfanyl substituted phthalonitriles [5].

The fragile ether bond between the macrocyclic core and oxo-substituents of AzaPc [4], may be one reason why this class of AzaPc has been ignored for many years. However, AzaPc which are substituted with bulky phenoxy groups, and which are soluble in most organic solvents, were obtained by direct synthesis as reported recently by Makhseed et al. [6,7]. These compounds are of potential interest for a variety of applications, and in particular as fluorophores since their red fluorescence falls within the visible spectrum.

* Corresponding author. Tel.: +47 97 10 39 26; fax: +47 73 59 42 56.
E-mail address: eva.morkved@chem.ntnu.no (E.H. Mørkved).

0277-5387/$ - see front matter © 2010 Elsevier Ltd. All rights reserved.
doi:10.1016/j.poly.2010.08.036

Pyridin-3-yloxy substituted Pc was studied for many years with the purpose of obtaining sensitizers applicable in photodynamic therapy (PDT) used in cancer treatment [8]. Recently some promising PDT sensitizers, namely cationic zinc complexes of octa(pyridin-3-yloxy)Pc have been reported [9]. We obtained related octa(pyridin-3-yloxy)ZnAzaPc, and some similarly substituted complexes [10] from reactions of substituted pyrazine-2,3-dicarbonitriles with Zn(quinoline)$_2$Cl$_2$. Due to low solubility in most organic solvents, there is limited potential for applications of those ZnAzPc. However, complexation of the peripheral pyridin-3-yloxy substituents with zinc(II) ions is an interesting possibility, since peripheral complexes with other metal ions might alter solubility and other important properties of these compounds.

We anticipate that further studies of aryloxy-substituted ZnAzaPc will give useful knowledge about these macrocycles. Indications of potential applications, including PDT, might follow. The Q-band, at 636 nm, of unsubstituted ZnAzaPc is considerably blue shifted compared to that of ZnPc (674 nm). Q-bands close to 700 nm are optimal for PDT sensitizers [2]. The thiophen-2-yl groups of octa(thiophen-2-yl)ZnAzaPc [11], induce a red shift to 673 nm in the Q-band of the UV–Vis spectrum, and also a higher intensity of this absorption. A lowering of energy can be effected both by a suitable extension of the delocalized electron system brought about by a sufficient degree of coplanarity between the thiophene substituents and the AzaPc core, and as well by polar interactions between the electron-donating thiophene rings and the electron-deficient macrocyclic system. Indications of the relative importance of polarity and coplanarity may be obtained from structure studies of pyrazine-2,3-dicarbonitriles **4a–d** (Scheme 1).

The purpose of our present study is to investigate how combinations of the peripheral substituents thiophen-2-yl, and ortho-substituted phenoxy groups influence the electronic properties of ZnAzaPc. These macrocycles are synthesized from substituted pyrazine-2,3-dicarbonitriles. The combination of one thiophen-2-yl group and one bulky aryloxy group on each pyrazine ring is expected to cause steric crowding, presumably favouring coplanarity between the thiophene and pyrazine rings, the aryloxy group being forced out of this plane. The crystal structures of monomers **4a** and **4b** (Scheme 1), are expected to give valuable information about these steric assumptions.

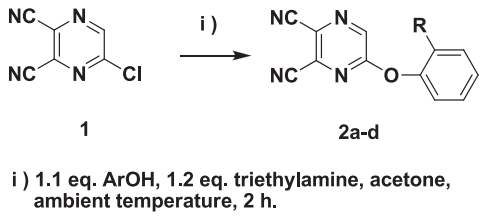

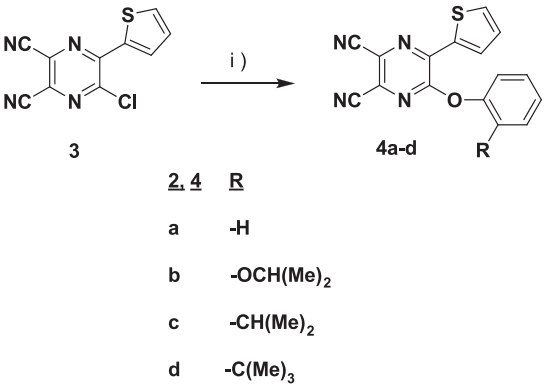

Scheme 1. Synthesis of unsymmetrically substituted pyrazine-2,3-dicarbonitriles **2a–d** and **4a–d**.

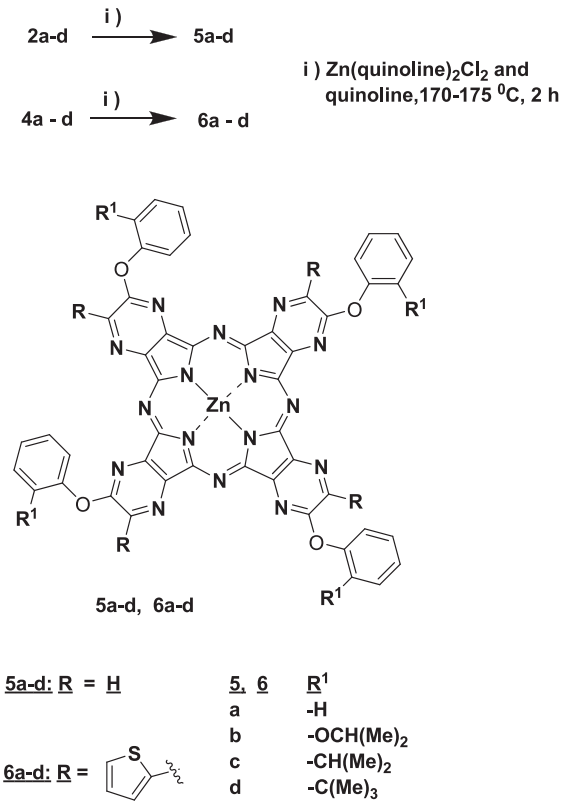

Scheme 2. Synthesis and structure of unsymmetrical aryloxy-substituted zinc azaphthalocyanines **5a–d** and **6a–d**. Only one structural isomer is shown for compounds **5** and **6**.

The tetrasubstituted ZnAzaPc **5a–d** (Scheme 2), are reference compounds, and aggregation certainly will be a problem with some of them. The phenoxy substituents of **5a** are not sufficiently bulky to cause steric crowding, whereas the ortho-isopropyloxy-, isopropyl- and *tert*-butyl-substituted phenoxy groups of respectively **5b–d**, may cause some steric crowding and thereby improve solubilities.

The octasubstituted complex **6a** (Scheme 2), is a reference for **6b–d** (Scheme 2), which are substituted with thiophen-2-yl groups and the same ortho-substituted phenoxy groups as in **5b–d**. The results of these investigations are expected to indicate if **6b–d** may be developed further; application as sensitizers for PDT would be one possibility.

2. Experimental

2.1. Materials and methods

Accurate mass determination with electron spray ionisation (ESI) was performed on an Agilent 6520 QTOF MS instrument equipped with a dual electrospray ion source. Samples of compounds **2** and **4**, dissolved in acetonitrile, were injected into the MS using an Agilent 1200 series HPLC, and analysis was performed as a flow injection analysis without any chromatographic step. MALDI-TOF mass spectra of compounds **5** and **6** were recorded on a Bruker Ultraflex III MALDI-TOF–TOF mass spectrometer operated in TOF mode. Each sample was dissolved in dichloromethane (DCM), spotted onto the target plate, airdried at ambient temperature and covered with the matrix solution which consisted of α-cyano-4-hydroxycinnamic acid, acetonitrile and trifluoroacetic acid. IR spectra were obtained on a Thermo Nicolet Nexus FT-IR spectrometer with a Smart Endurance reflexion cell. NMR spectra of **2**

and **4** were recorded on a Bruker Avance DPX 400 NMR spectrometer at 400.13 (^{1}H) and 100.61 MHz (^{13}C). NMR spectra of **5** and **6** were recorded on a Bruker Avance Digital 600 NMR spectrometer, fitted with a TCI cryoprobe, at 600.18 (^{1}H) and 150.92 MHz (^{13}C). Chemical shifts are given relative to internal tetramethyl silane (TMS) when $CDCl_3$ was used as solvent. Chemical shifts are calibrated relative to the DMSO signal at 2.50 ppm for ^{1}H, and 39.51 ppm for ^{13}C when DMSO-d_6 was used as solvent. The NMR pulse techniques COSY, ROESY, HSQC and HMBC were used to correlate ^{1}H and ^{13}C NMR signals for all new compounds. ^{13}C chemical shift values of **5** and **6** were determined by indirect methods (HSQC and HMBC) precluding the detection of ^{13}C nuclei not coupled to ^{1}H (usually more than three bonds away from ^{1}H). UV–Vis spectra were recorded on a Cary 50 UV–Vis spectrophotometer. Melting points were obtained on a Büchi 530 melting point apparatus and are uncorrected. Merck Kieselgel 60F 254 was used for thin layer chromatography (TLC) and Merck silica 63–200 μm was used for column chromatography. 2-Isopropyloxyphenol, 2-isopropylphenol and 2-*tert*-butylphenol were obtained from Aldrich. 5-Chloropyrazine-2,3-dicarbonitrile (**1**), was prepared as in [12], and 5-chloro-6-(thiophen-2-yl)pyrazine-2,3-dicarbonitrile (**3**), was prepared as in [13]. Compound **2a**, 5-phenoxypyrazine-2,3-dicarbonitrile, has been reported [12], but was prepared as described below.

2.2. Synthesis

2.2.1. Compounds **2a–d** and **4a–d**

*2.2.1.1. General procedure for the synthesis of compounds **2** and **4**.* Triethylamine (2.3 mmol) was added dropwise to a stirred solution of **1** or **3** (2 mmol) and phenol, 2-isopropyloxyphenol, 2-isopropylphenol or 2-*tert*-butylphenol (2.2 mmol), in acetone (20 ml). The reaction mixture was stirred at ambient temperature for 2 h, triethylammonium chloride, which separated from the reaction mixture, was removed by filtration. The solvent was removed from the filtrate, and the crude solid was chromatographed on silica with DCM to afford compounds **2a–d** and **4a–d**.

*2.2.1.2. 5-Phenoxypyrazine-2,3-dicarbonitrile (**2a**).* Yield of white powder, 0.37 g (77%), m.p. 148–152 °C, lit. [12] m.p. 150–151 °C. UV–Vis (DCM): λ_{max}, nm 255 (14 000). ^{1}H NMR ($CDCl_3$): δ, ppm *phenyl*: 7.16 (2H, *H2, H*6, m), 7.37 (1H, *H*4, m), 7.49 (2H, *H3, H*5, m), *pyrazine*: 8.67 (1H, *H*6, s). ^{13}C NMR ($CDCl_3$): δ, ppm 112.3 and 112.9 (*CN* at pyrazine C2, C3), *phenyl*: 120.9 (*C2, C*6), 127.1 (*C*4), 130.3 (*C3, C*5), 151.1 (*C*1), *pyrazine*: 126.8 (*C*2), 131.1 (*C*3), 140.2 (*C*6), 159.8 (*C*5).

*2.2.1.3. 5-(2-Isopropyloxyphenoxy)pyrazine-2,3-dicarbonitrile (**2b**).* Yield of white powder, 0.48 g (86%), m.p. 93–94 °C. ESIMS: *m/z* (% rel. int.) *Anal.* Calc. for $C_{15}H_{12}N_4O_2$ (M^+): 280.0960. Found: 280.0967. UV–Vis (DCM): λ_{max}, nm (ε, $M^{-1}\,cm^{-1}$) 297 (sh) (8700), 255 (17 000). IR: *v*, cm^{-1} 2983 (*CH*, w), 2238 (*CN*, w), 1494, 1431, 1358, 1333, 1281, 1252, 1187, 1105, 940, 771, 757. ^{1}H NMR ($CDCl_3$): δ, ppm 1.16 (6H, C*H*$_3$, d, *J* = 6.1 Hz), 4.54 (1H, C*H*$(CH_3)_2$, sept., *J* = 6.1 Hz), *phenyl*: 6.99 (1H, *H*5, m), 7.02 (1H, *H*3, m), 7.16 (1H, *H*6, dd, $J_{6,5}$ = 7.9 Hz, $J_{6,4}$ = 1.5 Hz), 7.29 (1H, *H*4, ddd, *J* = 8.5 Hz, *J* = 7.6 Hz, $J_{4,6}$ = 1,5 Hz), *pyrazine*: 8.63 (1H, *H*6, s). ^{13}C NMR ($CDCl_3$): δ, ppm 21.9 (*C*H$_3$), 70.9 (*C*H$(CH_3)_2$), 112.4 and 113.1 (*C*N at pyrazine C2, C3), *phenyl*: 114.9 (*C*3), 122.2 (*C*6), 127.9 (*C*4), 140.8 (*C*1), 148.7 (*C*2), *pyrazine*: 126.5 (*C*2), 131.2 (*C*3), 139.5 (*C*6), 159.8 (*C5).*

*2.2.1.4. 5-(2-Isopropylphenoxy)pyrazine-2,3-dicarbonitrile (**2c**).* Yield of white powder, 0.51 g (97%), m.p. 88–90 °C. ESIMS: *m/z* (% rel. int.) *Anal.* Calc. for $C_{15}H_{13}N_4O$ ($M+H^+$): 265.1084. Found: 265.1086. UV–Vis (DCM): λ_{max}, nm (ε, $M^{-1}\,cm^{-1}$) 255 (18 600), 295 (sh, 9000). IR: *v*, cm^{-1} 2969 (*CH*, w), 2240 (*CN*, w), 1557, 1530, 1433, 1360, 1339, 1213, 1173, 1108, 1077, 992, 935, 793, 755. ^{1}H NMR ($CDCl_3$): δ, ppm 1.20 (6H, C*H*$_3$, d, *J* = 6.9 Hz), 2.92 (1H, C*H*$(CH_3)_2$, sept. *J* = 6.9 Hz), *phenyl*: 7.00 (1H, *H*6, dd, $J_{6,5}$ = 8.0 Hz, $J_{6,4}$ = 1.2 Hz), 7.29 (1H, *H*5, app. td, *J* = 7.9 Hz, $J_{5,3}$ = 1.6 Hz), 7.35 (1H, *H*4, app. td, *J* = 7.6 Hz, $J_{4,6}$ = 1.2 Hz), 7.43 (1H, *H*3, dd, $J_{3,4}$ = 7.7 Hz, $J_{3,5}$ = 1.6 Hz), *pyrazine*: 8.68 (1H, *H*6, s). ^{13}C NMR ($CDCl_3$): δ, ppm 23.0 (*C*H$_3$), 27.5 (*C*H$(CH_3)_2$), 112.3 and 112.9 (*CN* at pyrazine C2 and C3), *phenyl*: 121.2 (*C*6), 127.4 (*C*5), 127.6 (*C*4), 127.7 (*C*3), 140.1 (*C*2), 148.6 (*C*1), *pyrazine*: 126.8 (*C*2), 131.4 (*C*3), 139.8 (*C*6), 160.1 (*C*5).

*2.2.1.5. 5-(2-tert-Butylphenoxy)pyrazine-2,3-dicarbonitrile (**2d**).* Yield of white powder, 0.33 g (59%), m.p. 115–117 °C. ESIMS: *m/z* (% rel. int.) *Anal.* Calc. for $C_{16}H_{14}N_4O$ (M^+): 278.1168. Found: 278.1173. UV–Vis (DCM): λ_{max}, nm (ε, $M^{-1}\,cm^{-1}$) 250 (15 400). IR: *v*, cm^{-1} 2965 (*CH*, w), 2236 (*CN*, w), 1556, 1530, 1433, 1362, 1340, 1264, 1180, 1108, 1083, 993, 932, 791, 757. ^{1}H NMR ($CDCl_3$): δ, ppm 1.33 (9H, C*H*$_3$, s), *phenyl*: 6.94 (1H, *H*6, dd, $J_{6,5}$ = 6.0 Hz, $J_{6,4}$ = 3.5 Hz), 7.29 (1H, *H*4, m), 7.30 (1H, *H*5, m), 7.51 (1H, *H*3, dd, $J_{3,4}$ = 6.0 Hz, $J_{3,5}$ = 3.6 Hz), *pyrazine*: 8.65 (1H, *H*6, s). ^{13}C NMR ($CDCl_3$): δ, ppm 30.4 (*C*H$_3$), 34.7 (*C*$(CH_3)_3$), 112.3 and 112.9 (*C*N at pyrazine C2 and C3), *phenyl*: 122.4 (*C*6), 127.0 (*C*4), 127.6 (*C*5), 128.2 (*C*3), *pyrazine*: 126.8 (*C*2),131.5 (*C*3), 140.0 (*C*6), 160.1 (*C*5).

*2.2.1.6. 5-Phenoxy-6-(thiophen-2-yl)pyrazine-2,3-dicarbonitrile (**4a**).* Yield of lemon yellow powder 0.53 g (87%), m.p. 243–244 °C. ESIMS: *m/z* (% rel. int.) *Anal.* Calc. for $C_{16}H_9N_4OS$ ($M+H^+$): 305.0492. Found: 305.0501. Calc. for $C_{16}H_{12}N_5OS$ ($M+NH_4^+$): 322.0757. Found 322.0757. UV–Vis (DCM): λ_{max}, nm (ε, $M^{-1}\,cm^{-1}$) 365 (18 500). IR: *v*, cm^{-1} 3079 (*CH*, w), 2235 (*CN*, w), 1513, 1486, 1401, 1384, 1234, 1178, 1157, 1063, 849, 806, 739, 690. ^{1}H NMR ($CDCl_3$): δ, ppm *thiophene*: 7.27 (1H, *H*4, dd, $J_{4,5}$ = 5.0, $J_{4,3}$ = 4.0) 7.78 (1H, *H*5, dd, $J_{5,4}$ = 5.0 Hz, $J_{5,3}$ = 1.1 Hz), 8.38 (1H, *H*3, dd, $J_{3,4}$ = 4.0 Hz, $J_{3,5}$ = 1.1 Hz), *phenyl*: 7.21 (2H, *H2, H*6, m), 7.52 (2H, *H3, H*5, m), 7.39 (1H, *H*4, m). ^{13}C NMR ($CDCl_3$): δ, ppm 112.9 and 113.1 (*CN* at pyrazine C2, C3), *thiophene*: 129.2 (*C*4), 134.2 (*C*3), 134.9 (*C*5), 136.3 (*C*2), *phenyl*: 121.4 (*C2, C*6), 127.1 (*C*4), 130.2 (*C3, C*5), 151.1 (*C*1), *pyrazine*: 126.1, 126.5 (*C2, C*3), 142.7 (*C*6), 154.9 (*C*5).

*2.2.1.7. 5-(2-Isopropyloxyphenoxy)-6-(thiophen-2-yl)pyrazine-2,3-dicarbonitrile (**4b**).* Yield 0.64 g (89%) of yellow powder, m.p. 157–158 °C. ESIMS: *m/z* (% rel. int.). *Anal.* Calc. for $C_{19}H_{14}N_4O_2S$ (M^+): 362.0837. Found: 362.0852. UV–Vis (DCM): λ_{max}, nm (ε, $M^{-1}\,cm^{-1}$) 370 (22 000). IR: *v*, cm^{-1} 3092 (*CH*, w), 2237 (*CN*, w), 1513, 1490, 1431, 1406, 1384, 1253, 1109, 937, 735. ^{1}H NMR ($CDCl_3$): δ, ppm 1.12 (6H, C*H*$_3$, d, *J* = 6.1 Hz), 4.53 (1H, C*H*$(CH_3)_2$, sept. *J* = 6.1 Hz), *thiophene*: 7.25 (1H, *H*4, dd, $J_{4,5}$ = 5.0 Hz, $J_{4,3}$ = 3.9 Hz), 7.76 (1H, *H*5, dd, $J_{5,4}$ = 5 Hz, $J_{5,3}$ = 1.0 Hz), 8.38 (1H, *H*3, dd, $J_{3,4}$ = 3.9 Hz, $J_{3,5}$ = 1.0 Hz), *phenoxy*: 7.03 (1H, *H*5, m), 7.04 (1H, *H*3, m), 7.22 (1H, *H*6, ddd, $J_{6,5}$ = 8.4 Hz, $J_{6,4}$ = 1.7 Hz, $J_{6,3}$ = 0.8 Hz), 7.30 (1H, *H*4, ddd, *J* = 8.3 Hz, *J* = 7.5 Hz, $J_{4,6}$ = 1.7 Hz). ^{13}C NMR ($CDCl_3$): δ, ppm 21.9 (*C*H$_3$), 71.0 (*C*H$(CH_3)_2$), 113.0 and 113.2 (*CN* at pyrazine *C2, C*3), *thiophene*: 129.1 (*C*4), 134.2 (*C*3), 134.5 (*C*5), 136.6 (*C*2), *phenoxy*: 114.9 (*C*3), 120.9 (*C*5), 122.5 (*C*6), 127.7 (*C*4), 141.2 (*C*1), 148.8 (*C*2), *pyrazine*: 126.16 (*C*2 or *C*3), 126.27 (*C*2 or *C*3), 142.3 (*C*6), 155.0 (*C*5).

*2.2.1.8. 5-[2-Isopropylphenoxy)]-6-(thiophen-2-yl)pyrazine-2,3-dicarbonitrile (**4c**).* Yield of yellow powder 0.63 g (91%), m.p. 209–210 °C. EIMS: *m/z* (% rel. int.). *Anal.* Calc. for $C_{19}H_{14}N_4OS$ (M^+): 346.0888. Found: 346.0877. UV–Vis (DCM): λ_{max}, nm (ε, $M^{-1}\,cm^{-1}$) 375 nm (24 000). IR: *v*, cm^{-1} 2956 (*CH*, w), 2236 (*CN*, w), 1518, 1406, 1383, 1336, 1234, 1165, 1077, 748, 720. ^{1}H NMR ($CDCl_3$): δ, ppm 1.21 (6H, C*H*$_3$, d, *J* = 6.9 Hz), 2.92 (1H, C*H*$(CH_3)_2$, sept.,

J = 6.9 Hz), *thiophene*: 7.28 (1H, *H*4, dd, $J_{4,5}$ = 5.0 Hz, $J_{4,3}$ = 4.0 Hz), 7.79 (1H, *H*5, dd $J_{5,4}$ = 5.0 Hz, $J_{5,3}$ = 1.1 Hz), 8.39 (1H, *H*3, dd, $J_{3,4}$ = 4.0 Hz, $J_{3,5}$ = 1.1 Hz), *phenoxy*: 7.02 (1H, *H*6, dd, $J_{6,5}$ = 8.0 Hz, $J_{6,4}$ = 1.2 Hz), 7.30 (1H, *H*5, app. td, *J* = 8 Hz, $J_{5,3}$ = 1.8 Hz), 7.37 (1H, *H*4, app. td, *J* = 7.5 Hz, $J_{4,6}$ = 1.2 Hz), 7.46 (1H, *H*3, $J_{3,4}$ = 7.5 Hz, $J_{3,5}$ = 1.8 Hz). ^{13}C NMR ($CDCl_3$): *δ*, ppm 23.3 (CH_3), 27.4 ($CH(CH_3)_2$), 112.9 and 113.1 (*CN* at pyrazine C2, C3), *thiophene*: 129.3 (*C*4), 134.0 (*C*3), 134.9 (*C*5), 136.4 (*C*2), *phenoxy*: 121.7 (*C*6), 127.4 (*C*5), 127.50 (*C*3), 127.55 (*C*4), 140.3 (*C*2), 148.6 (*C*1), *pyrazine*: 126.3 (*C*2 or *C*3), 126.4 (*C*2 or *C*3), 142.4 (*C*6), 155.2 (*C*5).

*2.2.1.9. 5-[2-tert-Butylphenoxy)]-6-(thiophen-2-yl)pyrazine-2,3-dicarbonitrile (**4d**).* Yield of yellow powder 0.53 g (73%), m.p. 214–216 °C. ESIMS: *m/z* (% rel. int.). *Anal.* Calc. for $C_{20}H_{17}N_4OS$ ($M+H^+$): 361.1118. Found: 361.1116. UV–Vis (DCM): λ_{max}, nm (ε, $M^{-1}\,cm^{-1}$) 375 nm (22 000). IR: *ν*, cm^{-1} 2953 (*CH*, w), 2235 (*CN*, w), 1509, 1429, 1403, 1384, 1232, 1168, 1080, 756, 731. ^{1}H NMR ($CDCl_3$): *δ*, ppm 1.33 (9H, CH_3, s), *thiophene*: 7.27 (1H, *H*4, dd, $J_{4,5}$ = 5.0 Hz, $J_{4,3}$ = 4.0 Hz), 7.78 (1H, *H*5, dd, $H_{5,4}$ = 5.0 Hz, $J_{5,3}$ = 1.1 Hz), 8.41 (1H, *H*3, dd, $J_{3,4}$ = 4.0 Hz, $J_{3,5}$ = 1.1 Hz), *phenoxy*: 6.87 (1H, *H*6, m), 7.30 (1H, *H*5, m), 7.31 (1H, *H*4, m), 7.55 (1H, *H*3, m). ^{13}C NMR ($CDCl_3$): *δ*, ppm 30.9 (CH_3), 34.7 ($C(CH_3)_3$), 112.8 and 113.1 (*CN* at pyrazine C2, C3), *thiophene*: 129.2 (*C*4), 133.9 (*C*3), 134.8 (*C*5), 136.3 (*C*2), *phenoxy*: 123.2 (*C*6), 126.9 (*C*4), 127.7 (*C*5), 128.3 (*C*3), 141.6 (*C*2), 150.4 (*C*1), *pyrazine*: 126.46 (*C*2 or *C*3), 126.52 (*C*2 or *C*3), 142.8 (*C*6), 155.8 (*C*5).

*2.2.2. Compounds **5a–d** and **6a–d***

*2.2.2.1. General procedure for the synthesis of compounds **5** and **6**.* Compound **2a–d** or **4a–d** (0.8 mmol), $Zn(quinoline)_2Cl_2$ (0.4 mmol) and freshly distilled quinoline (0.4 ml) were transferred to a round bottom flask. The stirred reaction mixture was flushed with nitrogen for 15 min at ambient temperature, and heated under nitrogen at 170–175 °C for 2 h. The dark semi-solid was sonicated with diethyl ether, and the collected dark solid was stirred with methanol (20 ml) for 1 h at ambient temperature in order to remove unreacted zinc salt. The crude solid was dissolved in a small amount of DCM and applied to a silica column. DCM eluted a small amount of yellow impurities. Compounds **5a** and **6a** were eluted with a mixture of DCM and DMF (9:1), compounds **5b** and **6b–d** were eluted with a mixture of DCM and acetone (4:1), whereas **5c** and **5d** were eluted with MeCN. The dark powders were dried at 0.1 mm Hg for 5 h at ambient temperature.

*2.2.2.2. [Tetra(phenoxy)-(octazaphthalocyaninato)]zinc(II) (**5a**).* Yield of dark blue powder 0.1 g (51%), UV–Vis (DMSO): λ_{max}, nm (ε, $M^{-1}\,cm^{-1}$) 635 (124 000), 575 (27 000), 360 (88 000). UV–Vis (pyridine): λ_{max}, nm (ε, $M^{-1}\,cm^{-1}$) 695 (20 000), 640 (64 000), 580 (19 000), 365 (66 160). IR: *ν*, cm^{-1} 3063 (*CH*, w), 1531, 1482, 1342, 1322, 1286, 1191, 1172 (sh), 1096, 1070, 985, 760, 747, 717, 688. ^{1}H NMR (DMSO-d_6): *δ*, ppm *phenyl*: 7.5–7.75 (*H*4, broad m), 7.65–7.85 (*H3, H*5, broad m), 7.7–8.0 (*H2, H*6, broad m), *pyrazine*: 9.1–9.45 (*H*6, four broad signals). ^{13}C NMR (DMSO-d_6): *δ*, ppm *phenyl*: 121.5–122 (*C2, C*5), 125–126 (*C*4), 129.5–130.5 (*C3, C*5), *pyrazine*: 137.5–138.5 (*C*6). MS (MALDI-TOF) *m/z* 953.20 [$M+H^+$]. *Anal.* Calc. for $C_{48}H_{24}N_{16}O_4Zn$: 952.146 (M), for $C_{48}H_{25}N_{16}O_4Zn$: 953.15 ($M+H^+$). The expected isotopic pattern for zinc was found at *m/z* (calcd. % rel. int.) 953.20 (52), 954.20 (57), 955.19 (30), 956.19 (39), 957.19 (20), 958.19 (5).

*2.2.2.3. 3[Tetra(2-isopropyloxyphenoxy)-(octazaphthalocyaninato)] zinc(II) (**5b**).* Yield of purple-black powder 0.13 g (53%). UV–Vis (DMSO): λ_{max}, nm (ε, $M^{-1}\,cm^{-1}$) 635 (121 000), 575 (28 000), 355 (85 000). IR: *ν*, cm^{-1} 2975 (*CH*, w), 1532, 1487, 1341, 1321, 11285, 1185, 1172, 1111, 1069, 986, 950, 740, 707. ^{1}H NMR (DMSO-d_6): *δ*, ppm 0.95–1.01 (CH_3, multiple d), 4.6–4.7 ($CH(CH_3)_2$, m), *phenyl*: 7.2–7.3 (*H*5, m), 7.35–7.45 (*H*3, m), 7.45–7.6 (*H*4, m), 7.55–7.75 (*H*6, m), *pyrazine*: 9.35–9.45 (*H*6, 3 sharp singlets). ^{13}C NMR (DMSO-d_6): *δ*, ppm 21–22 (CH_3), 69.5–70.5 ($CH(CH_3)_2$), *phenyl*: 115.5–116 (*C*3), 120.5–121.5 (*C*5), 123–123.5 (*C*6), 126–127 (*C*4), 142–143.5 (*C*1), 148.5–150 (*C*2), *pyrazine*: 137–138 (*C*6), 144–145 (*C*2), 160.5–161.5 (*C*5). MS (MALDI-TOF) *m/z* 1185.31 [$M+H^+$]. *Anal.* Calc. for $C_{60}H_{48}N_{16}O_8Zn$: 1184.313 (M), for $C_{60}H_{49}N_{16}O_8Zn$: 1185.317 ($M+H^+$). The expected isotopic pattern for zinc was found at *m/z* (calcd. % rel. int.) 1185.31 (65), 1186.31 (57), 1187.31 (37), 1188.31 (39), 1189.31 (25).

*2.2.2.4. [Tetra(2-isopropylphenoxy)-(octazaphthalocyaninato)]zinc(II) (**5c**).* Yield of purple-black powder 0.10 g (42%). UV–Vis (DMSO): λ_{max}, nm (ε, $M^{-1}\,cm^{-1}$) 635 (118 000), 575 (26 000), 355 (85 000).). IR: *ν*, cm^{-1} 2916, 2849 (*CH*, w), 1730, 1481, 1341, 1321, 1290, 1176, 1069, 985, 747, 618. ^{1}H NMR (DMSO-d_6): *δ*, ppm 1.3–1.4 (CH_3, multiple d), 3.3–3.45 ($CH(CH_3)_2$, m), *phenyl*: 7.4–7.65 (*H*4 and *H*5, m), 7.6–7.75 (*H*6, m), 7.65–7.75 (*H*3, m), *pyrazine*: 9.25–9.45 (*H*6 multiplets). ^{13}C NMR (DMSO-d_6): *δ*, ppm 22–23 (CH_3), 26.5–27.5 ($CH(CH_3)_2$), *phenyl*: 122–123 (*C*6), 126–127.5 (*C4, C*5), 126.5–127.5 (*C*3), 139.5–142 (*C*2), 149.5–151 (*C*1), *pyrazine*: 137–138 (*C*6). MS (MALDI-TOF) *m/z* 1121.38 [$M+H^+$]. *Anal.* Calc. for: $C_{60}H_{48}N_{16}O_4Zn$ 1120.33 (M), for $C_{60}H_{49}N_{16}O_4Zn$ 1121.34. The expected isotopic pattern for zinc was found at *m/z* (calcd. % rel. int.) 1121.4 (65), 1122.4 (57), 1123.4 (37), 1124.4 (39), 1125.4 (25), 1126.4 (8).

*2.2.2.5. [Tetra(2-tert-butylphenoxy)-(octazaphthalocyaninato)]zinc (II) (**5d**).* Yield of purple-black powder 0.07 g (33%). UV–Vis (DMSO): λ_{max}, nm (ε, $M^{-1}\,cm^{-1}$) 635 (135 000), 575 (30 000), 360 (94 000). IR: *ν*, cm^{-1} 2960 (*CH*, w), 1531, 1479, 1439, 1341, 1320, 1279, 1185, 1085, 1069, 984, 915, 875, 747, 718. ^{1}H NMR (DMSO-d_6): *δ*, ppm 1.5–1.6 (CH_3, 6 partly resolved singlets), *phenyl*: 7.1–7.9 (*H3, H4, H5, H*6, m), *pyrazine*: 9.25–9.45 (*H*6, multiplets). ^{13}C NMR (DMSO-d_6): *δ*, ppm 29.5–30.5 (CH_3), *phenyl*: 123–128 (*C4, C5, C*6), 127–128 (*C*3), 140–142 (*C*2), 151–152 (*C*1), *pyrazine*: 137.5–138.5 (*C*6). MS (MALDI-TOF) *m/z* 1177.43 [$M+H^+$]. *Anal.* Calc. for $C_{64}H_{56}N_{16}O_4Zn$: 1176.40 (M), for $C_{64}H_{57}N_{16}O_4Zn$: 1177.40 ($M+H^+$). The expected isotopic pattern for zinc was found at *m/z* (calcd. % rel. int.) 1176.4 (100), 1177.4 (69), 1178.4(57), 1179.4 (40), 1180.4 (39), 1181.4 (27).

*2.2.2.6. [Tetra(phenoxy)-tetra(thiophen-2-yl)-(octazaphthalocyaninato)]zinc(II) (**6a**).* Yield of black powder 0.09 g (35%). UV–Vis (DMSO): λ_{max}, nm (ε, $M^{-1}\,cm^{-1}$) 665 (111 000), 650, sh (103 000), 600 (33 000), 385 (106 000). IR: *ν*, cm^{-1} 3071 (*CH*, w), 1489, 1414, 1376, 1360, 1319, 1237, 1202 (sh), 1107, 1050, 962, 918, 843, 794, 744, 906, 686. ^{1}H NMR (DMSO-d_6): *δ*, ppm *phenyl*: 7.55–7.8 (*H*4, m), 7.65–7.85 (*H*3 and *H*5, m), 7.7–8.1 (*H*2 and *H6 m*), *thiophene*: 7.35–7.5 (*H*4, m), 8.0–8.2 (*H*5, m), 8.4–8.65 (*H*3, m). ^{13}C NMR (DMSO-d_6): *δ*, ppm *phenyl*: 121.5–122.5 (*C2, C*6), 125–126 (*C*4), 129.5–130.5 (*C3, C*5), *thiophene*: 128.5–129 (*C*4), 130.5–131.5 (*C*3), 131.5–132 (*C*5). MS (MALDI-TOF) *m/z* 1281.08 [$M+H^+$]. *Anal.* Calc. for $C_{64}H_{32}N_{16}O_4S_4Zn$: 1280.097 (M), for $C_{64}H_{33}N_{16}O_4S_4Zn$: 1281.100 ($M+H^+$). The expected isotopic pattern for zinc was found at *m/z* (calcd. % rel. int.) 1281.08 (69), 1282.08 (57), 1283.08 (40), 1284.09 (39), 1285.09 (27), 1286.09 (9), 1287.09 (5).

*2.2.2.7. [Tetra(2-isopropyloxyphenoxy)-tetra(thiophen-2-yl)(octazaphthalocyaninato)]zinc(II) (**6b**).* Yield of black powder 0.15 g (49%). UV–Vis (DMSO): λ_{max}, nm (ε, $M^{-1}\,cm^{-1}$) 660 (133 000), 595 (33 000), 385 (126 000). UV–Vis (pyridine): λ_{max}, nm (ε, $M^{-1}\,cm^{-1}$) 725 (11 000), 665 (124 000), 655, sh (119 000), 600 (32 000), 385 (126 000). IR: *ν*, cm^{-1} 2976 (*CH*, w), 1492, 1416, 1360, 1335,

1246, 1173, 1109, 1051, 952, 846, 792, 743, 709. ^{1}H NMR (DMSO-d_6): δ, ppm 0.91–1.01 (CH_3, 14 sharp signals (0.913–1.008) which are ascribed to 7 doublets with J = 5.5–6.0 Hz); 4.58–4.71 (CH(CH_3)$_2$, two overlapping septets; one septet centered at 4.61, and the other centered at 4.68, J = 5.4 Hz); *phenyl*: 7.25–7.4 (*H*5, m), 7.35–7.5 (*H*3, m), 7.5–7.7 (*H*4, m), 7.65–7.95 (*H*6, m), *thiophene*: 7.45–7.55 (*H*4, m), 8.1–8.2 (*H*5, m), 8.55–8.75 (*H*3, four d, 8.574, 8.606, 8.677, 8.706; all with J = 3.6 Hz). ^{13}C NMR (DMSO-d_6): δ, ppm 21–22 (CH_3), 69.5–70.5 (CH(CH_3)$_2$), *phenyl*: 115.5–116.5 (*C*3), 120.5–121.5 (*C*5), 123–124 (*C*6), 126–127.5 (*C*4), 143–144 (*C*1), 148–149.5 (*C*2), *thiophene*: 128.5–129 (*C*4), 131–131.5 (*C*3), 131.5–132 (*C*5), 139–140.5 (*C*2). MS (MALDI-TOF) *m/z* 1513.24 [M+H$^+$]. *Anal.* Calc. for $C_{76}H_{56}N_{16}O_8S_4Zn$: 1512.2641 (M), for $C_{76}H_{57}N_{16}O_8S_4Zn$: 1513.2675 (M+H$^+$). The expected isotopic pattern for zinc was found at *m/z* (calcd. % rel. int.) 1513.24 (82), 1514.24 (57), 1515.24 (47), 1516.24 (39), 1517.24 (32), 1518.24 (13), 1519.25 (7).

*2.2.2.8. [Tetra(2-isopropylphenoxy)-tetra(thiophen-2-yl)-(octazaphthalocyaninato)]zinc(II) (**6c**).* Yield of dark green powder 0.07 g (32%). UV–Vis (DMSO): λ_{max}, nm (ε, M^{-1} cm^{-1}) 660 (158 000), 600 (40 000), 385 (136 000). UV–Vis (pyridine): λ_{max}, nm (ε, M^{-1} cm^{-1}) 665 (159 000), 600 (38 000), 390 (131 000). IR: ν, cm^{-1} 2961, 2855 (*CH*, w), 1415, 1375, 1360, 1334, 1233, 1169, 1105, 1080, 1049, 963, 832, 793, 745, 704. ^{1}H NMR (DMSO-d_6): δ, ppm 1.3–1.5 (CH_3, five doublets of approximately equal intensity: (1.311, J = 6.6 Hz, 1.339 J = 6.78 Hz, 1.344 J = 6.8 Hz, 1.428 J = 6.8 Hz, 1.458 J = 6.8 Hz); 3.35–3.55 (CH(CH_3)$_2$, three septets: 3.362 J = 6.6 Hz, 3.479 J = 6.9 Hz, 3.526 J = 7 Hz); *phenyl*: 7.6–7.85 (*H*6, m); 7.5–7.85 (*H3, H4, H*5, m); *thiophene*: 7.5–7.6 (*H*4); 8.17–8.22 (*H*5, m), 8.55–8.75 (*H*3, four doublets: 8.589 J = 3.6 Hz, 8.624 J = 3.4 Hz, 8.715 J = 3.7 Hz, 8.742 J = 3.5 Hz). ROESY shows the following connections between the methyl ^{1}H signals of the isopropyl groups and the ^{1}H signals for thiophene-*H*3: 1.311/8.589; 1.339 and 1.344/8.715; 1.428/8.624; 1.458/8.742. MS (MALDI-TOF) *m/ z* 1449.306 [M+H$^+$]. *Anal.* Calc. for $C_{76}H_{56}N_{16}O_4S_4Zn$: 1448.28 (M), for $C_{76}H_{57}N_{16}O_4S_4Zn$: 1449.29 (M+H$^+$). The expected isotopic pattern for zinc was found at *m/z* (calcd. % rel. int.) 1449.3 (82), 1450.3 (57), 1451.3 (47), 1452.3 (39), 1453.3 (32), 1454.3 (13), 1455.3 (6).

*2.2.2.9. [Tetra(2-tert-butylphenoxy)-tetra(thiophen-2-yl)-(octazaphthalocyaninato)]zinc(II) (**6d**).* Yield of dark green powder 0.10 g (42%). UV–Vis (DMSO): λ_{max}, nm (ε, M^{-1} cm^{-1}) 660 (120 000), 600 (30 000), 390 (100 000). UV–Vis (pyridine): λ_{max}, nm (ε, M^{-1} cm^{-1}) 665 (139 000), 600 (35 000), 390 (119 000)%. IR: ν, cm^{-1} 2955 (*CH*, w), 1519 (w), 1415, 1359, 1333, 1248, 1231, 1174, 1106, 1082, 1049, 962, 821, 793, 746, 706. ^{1}H NMR (DMSO-d_6): δ, ppm 1.46–1.58 (CH_3, eight singlets of approximately equal intensity: 1.463, 1.468, 1.506, 1.511, 1.528, 1.532, 1.572, 1.575); *phenyl*: 7.55–7.7 (*H4, H*5, m), 7.6–7.85 (*H*6, m), 7.7–7.8 (*H*3, m), *thiophene*: 7.5–7.6 (*H*4, m), 8.15–8.25 (*H*5, m), 8.55–8.75 (*H*3, four doublets of equal intensity: (8.562 J = 3.5 Hz, 8.600 J = 3.3 Hz, 8.691 J = 3.4 Hz, 8.728 J = 3.3 Hz). ROESY showed the following connection between the *tert*-butyl ^{1}H signals and the ^{1}H signals of thiophene-*H*3: 1.463, 1.468/8.562; 1.506, 1.511/8.691; 1.528, 1.532/8.600; 1.572, 1.575/8.728. ^{13}C NMR (DMSO-d_6): δ, ppm 30–31 (CH_3, ca. 34 (C(CH_3)$_3$), *phenyl*: 124–125 (*C*6), 125–128 (*C4, C*5), 127–128 (*C*3), 141 (*C*2), 151–152 (*C*1), *thiophene*: 128.9 (*C*4), 130–131.1 (*C*3, HSQC connection between four ^{1}H and ^{13}C signals: 8.728/131.1, 8.691/130.0, 8.600/131.0, 8.562/130.9), ca. 132 (*C*5), ca. 140 (*C*2). MS (MALDI-TOF) *m/z* 1505.368 [M+H$^+$]. *Anal.* Calc. for $C_{80}H_{64}N_{16}O_4S_4Zn$: 1504.35 (M), for $C_{80}H_{65}N_{16}O_4S_4Zn$ 1505.35 (M+H$^+$). The expected isotopic pattern for zinc was found at *m/z* (calcd. % rel. int.) 1505.4 (87), 1506.4 (57), 1507.4 (50), 1508.4 (39), 1509.4 (33), 1510.4 (14), 1511.4 (6).

2.3. X-ray crystallographic studies

Compounds **4a** and **4b** were synthesized as described in paragraphs 2.2.1.1. (general), 2.2.1.6. (**4a**) and 2.2.1.7. (**4b**). Single crystals, in both cases of light yellow colour, were obtained by slow evaporation of solutions in acetonitrile, for **4b** a small admixture of dichloromethane proved useful. Data for both compounds were collected with a Nonius KappaCCD diffractometer, equipped with a rotating anode generator. Programs used for the various crystallographic operations were, for data collection: COLLECT [14], data reduction: Denzo-SMN [15], absorption correction: Denzo [16], structure solution by direct methods: SHELXS-97 [17], structure refinement: SHELXL-97 [18], and graphics: ORTEP-3 [19].

A summary of crystallographic parameters, and parameters for data collections and structure refinements is given in Table 1.

Compound **4a** showed disorder in the thiophene ring comprising two distinct sites, one major (*A* ring) and one minor (*B* ring) site. The occupancies of the two rings refined to 0.748 (2), and 0.252 (2), respectively, corresponding to a ratio A:$B \sim 3$:1. For the refinement the atomic positions C(11A) and C(11B) were constrained to coincide, atomic displacement parameters (ADPs) of the other *B* atoms were made equal to those for the parent *A* atoms, and a weak restraint was imposed on the bond lengths of the *B* ring.

No restraints were required in the refinement of structure **4b**.

Non-H atoms were refined anisotropically in both structures. The H atoms were calculated and refined as riding atoms using isotropic ADPs. Full-matrix least-squares refinements were based on F^2 using all reflections.

Table 2 contains a selection of structure data.

3. Results and discussion

3.1. Synthesis and characterization

3.1.1. Precursors **2a–d** and **4a–d**

The trisubstituted 5-(aryloxy)pyrazine-2,3-dicarbonitriles (**2a–d**), i.e. 5-phenoxypyrazine-2,3-dicarbonitrile (**2a**), 5-(2-isopropyloxyphenoxy)pyrazine-2,3-dicarbonitrile (**2b**), 5-(2-isopropylphenoxy)pyrazine-2,3-dicarbonitrile (**2c**) and 5-(2-*tert*-butylphenoxy) pyrazine-2,3-dicarbonitrile (**2d**), were obtained in 59–97% yields from reactions of 5-chloropyrazine-2,3-dicarbonitrile (**1**) with phenol, 2-isopropyloxyphenol, 2-isopropylphenol or 2-*tert*-butylphenol, and triethylamine in acetone at ambient temperature (Scheme 1). Compounds **4a–d**, namely 5-phenoxy-6-(thiophen-2-yl) pyrazine-2,3-dicarbonitrile (**4a**), 5-(2-isopropyloxyphenoxy)-6-(thiophen-2-yl)pyrazine-2,3-dicarbonitrile (**4b**), 5-(2-isopropylphenoxy)-6-(thiophen-2-yl)-2,3-dicarbonitrile (**4c**) and 5-(2-*tert*-butylphenoxy)-6-(thiophen-2-yl)pyrazine-2,3-dicarbonitrile (**4d**), were obtained in 73–91% yields by the same procedure (Scheme 1).

Melting points of aryloxy-substituted compounds **2** are influenced by the R-substituents on the phenoxy groups (Scheme 1). Thus, the isopropyloxy group of **2b** lowers the melting point from 150 °C for **2a** to 93 °C for **2b**. A similar shift is observed for compounds **4**, i.e. **4a** melts at 243 °C and **4b** at 157 °C. Good solubility in organic solvents, and absence of aggregation, are expected features of low-melting compounds. The isopropyloxy groups of **2b** and **4b** appear to be more effective than the non-polar isopropyl- or *tert*-butyl groups in this respect.

The thiophen-2-yl substituents of compounds **4** are expected to extend the conjugated system of compounds **2**. UV–Vis spectra confirm the anticipated effect; the strongest absorptions of compounds **2** are found at 255 nm, whereas the corresponding absorptions of **4** are observed at 365–370 nm.

Table 1
Summary of crystallographic parameters, data acquisition and refinement data for **4a** and **4b**.

Compound	**4a**	**4b**
Composition	$C_{16}H_8N_4OS$	$C_{19}H_{14}N_4O_2S$
Formula weight, M_r	304.32	362.40
Mp (K)	516–517	430-431
Crystal system, space group	monoclinic, $P2_1/n$	monoclinic, $P2_1/n$
T (K)	223(2)	223(2)
Unit cell dimensions		
a (Å)	6.8886(2)	5.6855(1)
b (Å)	20.2377(5)	20.6918(4)
c (Å)	10.0773(3)	14.7598(3)
β (°)	95.031(1)	98.547(1)
V (Å^3)	1399.46(7)	1717.11(6)
D_{calc} (Mg m^{-3})	1.444	1.402
Molecules per unit cell, *Z*	4	4
λ (Å)	0.71073	0.71073
Crystal size (mm)	0.42 × 0.20 × 0.08	0.30 × 0.17 × 0.15
Absorption coefficient, μ (mm^{-1})	0.238	0.210
Transmission, minimum/maximum	0.907/0.981	0.940/0.969
Scan modes	ω and φ	ω and φ
Resolution, s_{max} $\sin\theta/\lambda$ (Å^{-1})	0.66	0.66
Completeness within s_{max} (%)	96.6	97.5
Total no. of reflections/unique reflections	9161/3254 [R_{merge}(all) = 0.059]	10112/3999 [R_{merge}(all) = 0.047]
Unique reflections with $F^2 > 2\sigma(F^2)$ (NO)	2573	3171
No. of reflections/restraints/variables (NV)	3254/10/212	3999/0/237
Final *R* indices ($F^2 > 2\sigma(F^2)$)	$R(F)$ = 0.0687; $wR(F^2)$ = 0.1482	$R(F)$ = 0.0631; $wR(F^2)$ = 0.1358
Final *R* indices (all data)	$R(F)$ = 0.0877; $wR(F^2)$ = 0.1604	$R(F)$ = 0.0811; $wR(F^2)$ = 0.1494
Weight parameters w_A and w_B	0.0337/1.58	0.0342/2.16
Goodness-of-fit (GOF) on F^2	1.091	1.077
Extrema in residual electron density (e·Å^{-3})	−0.25/0.30	−0.36/0.28

$w = 1/[\sigma^2(F_o^2) + (w_A * P)^2 + w_B * P]$ where $P = (\text{Max}(F_o^2, 0) + 2 * F_c^2)/3$.
$R(F) = \Sigma||F_o| - |F_c||/\Sigma|F_o|$.
$wR(F^2) = \{\Sigma[w(F_o^2 - F_c^2)^2]/\Sigma[w(F_o^2)^2]\}^{1/2}$.
$\text{GOF} = [\Sigma w(F_o^2 - F_c^2)^2/(\text{NO} - \text{NV})]^{1/2}$.

3.1.2. Zinc(II) azaphthalocyanines *5a–d* and *6a–d* obtained from cyclotetramerization of precursors *2a–d* and *4a–d*

One well-known method for direct synthesis of zinc(II) complexes of phthalocyanines, or azaphthalocyanines, is to heat quinoline solutions of zinc(II) acetate and substituted phthalonitriles or pyrazine-2,3-dicarbonitriles. However, since reactions of zinc(II) acetate and quinoline with pyridin-3-yloxy substituted pyrazine-2,3-dicarbonitriles resulted in extensive decomposition [10], we decided to use the salt Zn(quinoline)$_2$Cl$_2$, prepared from zinc(II) chloride and quinoline, for cyclotetramerizations of compounds **2** and **4**. The synthesis and structure of ZnAzaPc **5** and **6** is shown in Scheme 2. A moderate reaction temperature, i.e. 170–175 °C, was considered best for these cyclotetramerizations in order to suppress possible loss of the aryloxy substituents. However, due to high melting points of thiophen-2-yl substituted monomers **4a** (243 °C) and **4d** (214 °C), a small amount of quinoline was added to each reaction mixture in order to keep reaction conditions constant for these cyclotetramerizations. Thus, precursors **2** and **4** were heated with Zn(quinoline)$_2$Cl$_2$ and a small amount of quinoline for 2 h at 170–175 °C. ZnAzaPc **5** and **6** were obtained in reasonable yields after purification by chromatography on silica. In order to compensate for the electron-donating, and expected deactivating effect of thiophene, longer reaction times were tested for reactions of **4**. However, compounds **6** were not obtained in higher yields. The immediate appearance of yellow-orange, then reddish-brown colours for reaction solutions of **4,** indicate some decomposition or polymerisation. The cyclotetramerizations of **2**, however, immediately gave green-blue coloured solutions that turned dark within a couple of minutes.

3.1.3. UV–Vis absorption of macrocycles *5* and *6*

The peripheral substituents of compounds **5** and **6** will induce shifted UV–Vis absorptions compared to unsubstituted ZnAzaPc.

Noncoplanarity is expected between the aryloxy groups and the macrocyclic core. Consequently, these substituents should provide space between stacked macrocycles, leading to less aggregation and enhanced solubility. Due to their smaller steric requirements the unsubstituted phenoxy groups of **5a** and **6a** should have limited influence on aggregation, and these compounds were synthesized as references for **5b–d** and **6b–d**, respectively. The bulky, ortho-substituted phenoxy groups of **5b–d** and **6b–d** are expected to increase the distance between stacked macrocycles, and to be more effective in preventing aggregation. The absence of aggregation would become evident from both shape and position of the Q-bands of these 18-π electron macrocycles.

Thiophene substituents of compounds **6** were introduced in order to induce red-shifted Q-bands; i.e. thiophene and the macrocycle are expected to form an extended π-electron system. Q-bands at 660–665 nm were measured for DMSO solutions of compounds **6**, and this Q-band red-shift of 25–30 nm is ascribed to the thiophene substituents. The shape is somewhat different for the absorption spectra of compounds **6** and **5**. A descending line is observed in the 400–500 nm area for compounds **5**, whereas a long shoulder appears in the same area for compounds **6**, as shown in Fig. 1, for **5b** and **6b**. Consequently, solutions of **5** are blue-green, but solutions of compounds **6** are grass-green in most organic solvents.

A third factor, which would presumably also affect UV–Vis absorptions of the unsymmetrically substituted macrocycles **5** and **6**, is the formation of structural isomers. Broad and unsymmetric Q-bands would be expected for this reason, as well as from aggregation. In fact, the Q-bands for all the DMSO solutions of **5** and **6** are slightly rounded and asymmetric, indicating the presence of more than one structural isomer as shown for **5b** and **6b** (Fig. 1).

Table 2
Selected bond lengths (Å) and bond angles (°) with esd's in parentheses for **4a** and **4b**.

	4a	4b
Bond lengths		
C(1)–C(2)	1.432 (4)	1.436 (3)
C(2)–N(3)	1.305 (3)	1.310 (3)
N(3)–C(4)	1.343 (3)	1.343 (3)
C(4)–C(5)	1.378 (4)	1.383 (3)
C(5)–N(6)	1.344 (3)	1.344 (3)
N(6)–C(1)	1.330 (3)	1.329 (3)
C(4)–C(41)	1.443 (4)	1.437 (3)
C(41)–N(42)	1.136 (4)	1.141 (3)
C(5)–C(51)	1.446 (4)	1.442 (3)
C(51)–N(52)	1.133 (4)	1.141 (3)
C(1)–C(11)	1.448 (4)/1.448 (4)*	1.451 (3)
C(11)–S(12)	1.729 (3)/1.705 (5)*	1.719 (3)
S(12)–C(13)	1.721 (5)/1.729 (11)*	1.698 (3)
C(13)–C(14)	1.356 (5)/1.358 (9)*	1.350 (4)
C(14)–C(15)	1.356 (8)/1.356 (12)*	1.417 (4)
C(15)–C(11)	1.358 (6)/1.343 (10)*	1.388 (3)
C(2)–O(21)	1.336 (3)	1.342 (3)
O(21)–C(21)	1.416 (3)	1.410 (3)
C(21)–C(22)	1.360 (4)	1.387 (4)
C(22)–C(23)	1.416 (6)	1.396 (4)
C(23)–C(24)	1.357 (6)	1.375 (4)
C(24)–C(25)	1.348 (6)	1.376 (4)
C(25)–C(26)	1.376 (4)	1.383 (4)
C(26)–C(21)	1.361 (4)	1.374 (4)
C(22)–O(22)		1.366 (3)
O(22)–C(27)		1.455 (3)
C(27)–C(28)		1.497 (4)
C(27)–C(29)		1.502 (4)
Bond angles		
C(2)–C(1)–N(6)	118.9 (2)	119.1 (2)
C(1)–C(2)–N(3)	123.3 (2)	123.0 (2)
C(2)–N(3)–C(4)	116.6 (2)	116.6 (2)
N(3)–C(4)–C(5)	121.6 (3)	121.7 (2)
C(4)–C(5)–N(6)	121.9 (2)	121.7 (2)
C(5)–N(6)–C(1)	117.8 (2)	117.9 (2)
C(4)–C(41)–N(42)	178.8 (3)	177.2 (3)
C(5)–C(51)–N(52)	178.3 (3)	177.9 (3)
N(6)–C(1)–C(11)	117.3 (2)/117.3 (2)*	116.9 (2)
C(2)–C(1)–C(11)	123.8 (2)/123.8 (2)*	124.0 (2)
C(1)–C(11)–S(12)	118.4 (2)/123.1 (2)*	117.9 (2)
C(1)–C(11)–C(15)	133.7 (3)/127.4 (6)*	131.1 (2)
C(15)–C(11)–S(12)	107.9 (3)/109.4 (6)*	111.1 (2)
C(11)–S(12)–C(13)	91.4 (2)/90.6 (7)*	92.0 (1)
S(12)–C(13)–C(14)	112.2 (5)/112.2 (12)*	112.3 (2)
C(13)–C(14)–C(15)	110.6 (6)/109.9 (13)*	113.3 (2)
C(14)–C(15)–C(11)	117.9 (6)/117.6 (10)*	111.4 (2)
C(2)–O(21)–C(21)	118.7(2)	118.2 (2)
C(26)–C(21)–C(22)	123.1 (3)	122.1 (2)
C(21)–C(22)–C(23)	117.0 (4)	118.0 (3)
C(22)–C(23)–C(24)	119.5 (4)	120.1 (3)
C(23)–C(24)–C(25)	121.7 (4)	120.8 (3)
C(24)–C(25)–C(26)	120.0 (4)	120.1 (3)
C(25)–C(26)–C(21)	118.6 (3)	118.9 (3)

* First value applies for A ring (major), second value for B ring (minor). C(11A) and C(11B) are constrained to superpose.

3.1.4. NMR analysis of macrocycles *5* and *6*

Whereas dilute solutions were used for UV–Vis spectroscopy, the NMR solutions had to be far more concentrated (approximately 10^{-3} M), and therefore aggregation became a problem. Compounds **5** and **6** are soluble in chloroform, dichloromethane and DMSO, but only DMSO-d_6 was used for the NMR analyses of **5** and **6** in order to minimise aggregation. Identifications of the ^{1}H NMR and corresponding ^{13}C NMR signals were made by using the pulse techniques COSY, ROESY, HSQC and HMBC. Multiple ^{1}H NMR signals may occur for several of the hydrogen atoms of compounds **5** and **6** due to the possibility of structural isomerism. With two

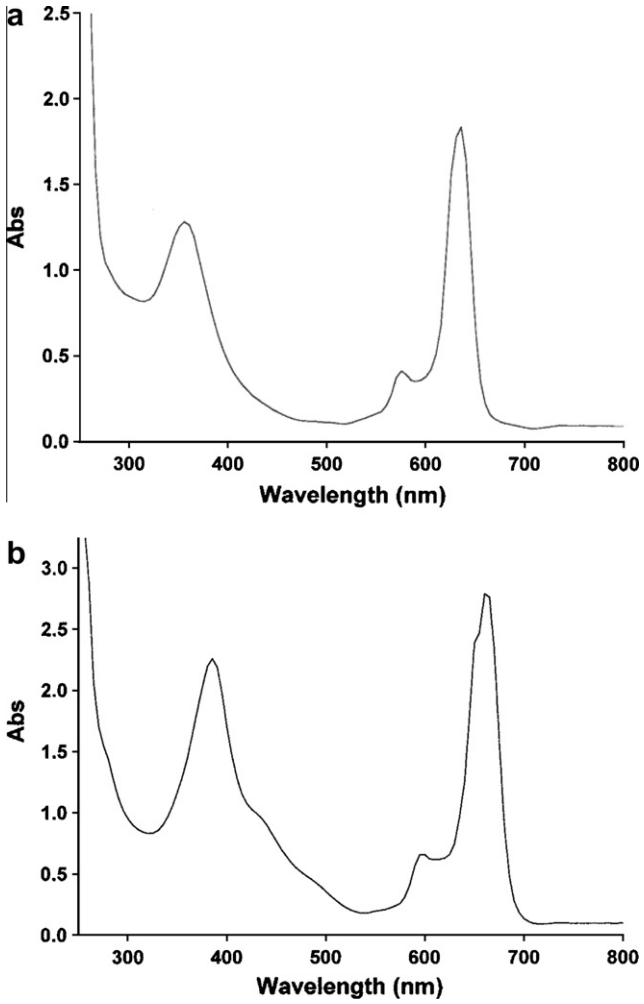

Fig. 1. (a) UV–Vis absorption spectrum of compound **5b** dissolved in DMSO, concentration 0.018 mg/ml DMSO (1.5×10^{-5} M). Blue-green solution. (b) UV–Vis absorption spectrum of compound **6b** dissolved in DMSO, concentration 0.024 mg/ml DMSO (1.7×10^{-5} M). Grass-green solution.

different orientations of each of the four constituents of macrocycles **5** and **6**, there is a total of 16 (2^4) possible combinations. By drawing all combinations it is obvious that there are four possible isomers and in total eight different sets of chemical shifts, e.g. pyrazine-*H*6 signals of **5**. If the macrocycles are arbitrarily formed, the eight different sets of NMR signals are expected to be equally intense.

Compounds **5**. The peripheral pyrazine-*H*6 atoms of compounds **5a–d** show the following: ^{1}H NMR signals: **5a**: 9.1–9.45 ppm (two broad and two sharp singlets), **5b**: 9.35–9.45 ppm (three sharp singlets), **5c**: 9.25–9.45 ppm (four partly overlapping broad singlets), **5d**: 9.25–9.45 ppm (three broad singlets). We conclude from these observations that aggregation is the origin of the broad signals of **5a**, **5c** and **5d**, whereas there is no evidence of aggregation for **5b**. Apparently each of compounds **5a–d** is formed as several structural isomers since several ^{1}H NMR singlets were observed for their pyrazine-*H*6 atoms. ^{1}H NMR signals of the phenoxy ortho-substituents (R) of compounds **5b–d** are informative as well. About seven doublets at 0.95–1.0 ppm are observed for the isopropyloxy-methyl groups of **5b**, and a multiplet at 4.6–4.7 ppm for the isopropyloxy-methine hydrogens. The ^{1}H signals from the isopropyl groups of **5c** are several apparent doublets at 1.3–1.4 ppm for the methyl hydrogens, and a multiplet at 3.3–3.45 ppm for the methine hydrogens. The methyl hydrogens of the *tert*-butyl groups of **5d** appear as six, partly unresolved, singlets at 1.5–1.6 ppm.

Compounds **6.** ^{1}H NMR signals similar to those of **5b** are observed for the isopropyloxy groups of **6b**. Seven doublets at 0.91–1.01 ppm (J = 5.5–6.0 Hz), are observed for the respective methyl groups, and two overlapping septets are observed at 4.58–4.71 ppm (J = 5.4 Hz), for the methine hydrogens of **6b**. The thiophene-*H*3 signals of **6b** are observed as four doublets at 8.55–8.75 ppm (J = 3.6 Hz). Similar observations are made for **6c** where the methyl signals of the isopropyl groups are five doublets at 1.3–1.5 ppm (J = 6.6–6.8 Hz). The methine signals of the isopropyl groups are three septets at 3.35–3.55 ppm (J = 6.6–7 Hz). The thiophene-*H*3 signals are four doublets of about equal intensities at 8.55–8.75 ppm (J = 3.4–3.7 Hz). The ROESY experiment showed NOE transfer between the isopropyl-methyl protons and the *H*3 protons of thiophene, linking together chemical shifts belonging to the same isomer. Eight sharp ^{1}H NMR singlets are observed at 1.46–1.58 ppm for the *tert*-butyl-methyl hydrogens of **6d**, and thiophene-*H*3 signals appear as four doublets of about equal intensity at 8.55–8.75 ppm, (J = 3.3–3.5 Hz). The ROESY pulse technique showed close spatial connection between the phenoxy-*tert*-butyl groups and the thiophene-*H*3 hydrogens, analogous to the connection between the isopropyl group and the thiophene-*H*3 hydrogens of **6c**.

3.1.5. Mass spectrometry of macrocycles *5* and *6*

Mass spectrometry (MALDI-TOF) of compounds **5** and **6** show the calculated molecular ions with the expected isotopic clusters characteristic of zinc. The compounds were dissolved in dichloromethane, spotted onto the target plate and dried at ambient temperature before being covered with matrix and injected into the spectrometer.

3.1.6. Crystal structures of compounds *4a* and *4b*

Similar projections of the two molecules with the atomic numbering are shown in Fig. 2(a) and (b). Common to both are three rings, pyrazine, thiophene and a phenoxy ring, denoted in the following as rings *I*, *II* and *III*, respectively. The disorder of the thiophene rings of **4a** can be described as a 180° rotational isomerism defined by rings *A* and *B* that occur in the ratio 3:1. The juxtaposed rings are nearly coplanar. For the calculations of conformation involving ring *II* in **4a** we have used the more precise atomic coordinates of the major *A* ring. Rings *I* and *II* are almost exactly coplanar in **4a**, the interplanar angle being ~3°. Ring *III* makes an angle of about 83° with ring *II*, thus there is a nearly orthogonal arrangement of the rings in this structure. In **4b** ring *II* is rotated slightly clockwise about the C(1)–C(11) bond vector making the interplanar angle between *I* and *II* about 12°. Ring *III* is rotated more away from orthogonality with ring *II* than in **4a**, the interplanar angle between *III* and *II* being ~69°. The combined effect of these rotations is to relieve close contacts between ring *II* and the isopropyloxy group of ring *III*. Fig. 3(a) and (b) illustrate the

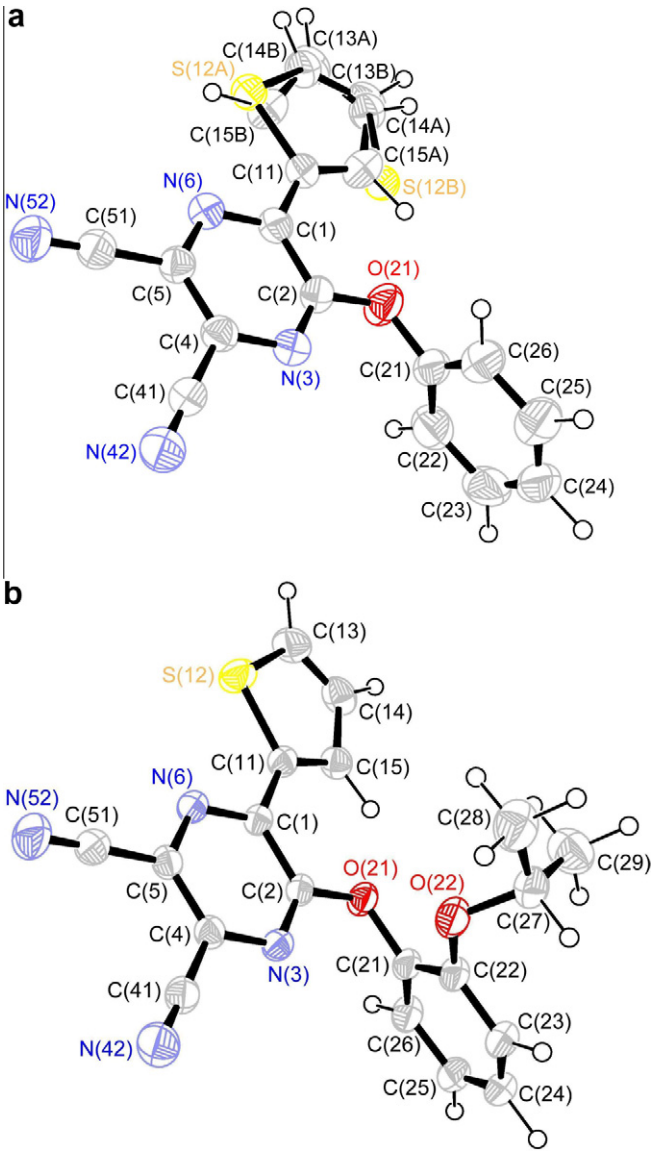

Fig. 2. Molecular conformation of compounds **4a** in (a) and **4b** in (b) with atomic numbering. Disorder in **4a** corresponds to a 180° rotational isomerism in the thiophene ring. The ratio of rings A to B is 3:1. ADP ellipsoids represent a 50% probability.

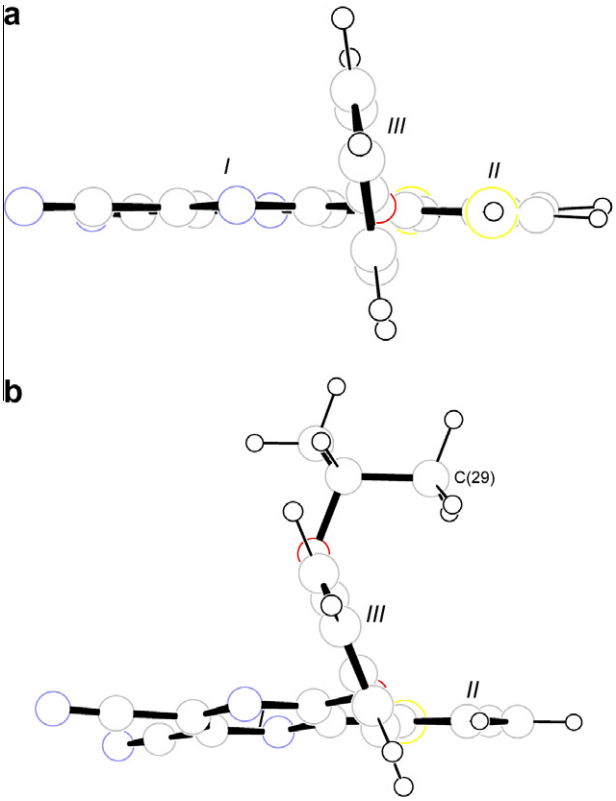

Fig. 3. Comparison of the orientation of the three rings *I*, *II* and *III*, in **4a** in (a) and **4b** in (b). The planes of the thiophene (*II*) and the phenoxy (*III*) rings are both very nearly parallel to the line of projection in the figures.

differences in conformation between structures **4a** and **4b**. In these figures the planes of both rings *II* and *III* are very nearly parallel to the line of projection.

Atoms O(21) and H(15) are nearly eclipsed in both structures, the distance between these atoms is 2.26 Å in **4a** and 2.30 Å in **4b**. In the disordered **4a** structure O(21) also makes a very short contact, 2.68 Å, with S(12B) of the minor thiophene ring. It appears that both the oxygen atom O(22) and the C(29) methyl of the isopropyloxy group in **4b** would make short contacts with a S atom vicinal to the phenoxy oxygen O(21) and therefore hinder 180° rotational isomerism, i.e. disorder.

Contacts involving H have been calculated with C(sp^2)–H bonds normalised at 1.09 Å, C(sp^3)–H bonds at 1.10 Å.

A selection of bonding parameters for the two structures is listed in Table 2. The geometry of the two *I* rings is very similar. With one exception the deviations between corresponding bond lengths and bond angles are $\leqslant$2 esd. The differences in rings *II* are larger, average and maximum values for bond lengths are 0.026 and 0.061 Å, respectively, parent differences in the bond angles are 2.6° and 6.5°. The increased disparity may be ascribed largely to difficulties in modelling and refining disorder in ring *II* of **4a**. The magnitudes of the discrepancies are largest for parameters involving C(14A/B), C(15A/B) and C(11). The bond lengths in **4b** are in overall better agreement with average values given for unsubstituted thiophene rings, C(sp^2)–S bonds: 1.712 Å, C(sp^2)–C(sp^2) double bonds: 1.362 Å, and the C(sp^2)–C(sp^2) single bond: 1.424 Å [20]. Comparing bonding parameters of rings *III* (note opposite numbering of C atoms in **4a** and **4b**) one finds for the average and maximum deviations in bond lengths 0.023 and 0.033 Å, respectively, parent values for the bond angles are 0.85° and 1.9°.

4. Conclusion

The choice of methods for syntheses of aryloxy substituted ZnAzaPc is limited by the observed replacement of aryloxy groups by strong nucleophiles, such as alkoxy ions, which often are used for cyclotetramerizations. The reagent Zn(quinoline)$_2$Cl$_2$ was used for direct syntheses of tetra(aryloxy) substituted ZnAzaPc **5a–d** and tetra(aryloxy)-tetra(thiophen-2-yl) substituted **6a–d**. These compounds were obtained in 30–50% yields and were mixtures of structural isomers. Both UV–Vis absorption and ^{1}H NMR spectrometry were used to determine aggregation of the reference compounds **5a–d**. Extensive aggregation was found for **5a**, which is substituted with peripheral phenoxy groups. Less aggregation, and improved solubility was found for compounds **5b–d**, that are substituted with ortho-functionalized phenoxy groups. However, Q-band absorptions were observed at the same wavelength (635 nm), for compounds **5a–d**, confirming insignificant conjugation between the aryloxy groups and the macrocycle of compounds **5**. Compound **6a** shows considerable aggregation, as anticipated. In other words, unsubstituted phenoxy substituents are not sufficiently bulky to prevent aggregation, even in the presence of neighbouring thiophen-2-yl groups.

The targeted octa-substituted compounds **6b–d** are quite soluble in organic solvents, and resist aggregation to a large degree, presumably due to the close vicinity of bulky ortho-substituted phenoxy groups and thiophen-2-yl substituents. ^{1}H NMR analysis of the sharp and well resolved alkyl signals of compounds **6b–d** indicate that polar isopropyloxy substituents of **6b** prevent aggregation slightly more efficiently than the isopropyl or *tert*-butyl groups of **6c** and **6d** do. The same conclusion is made by analysis of the ^{1}H NMR signals from the thiophene-*H*3 atoms of these compounds. The lower tendency for aggregation of compound **5b** compared to **5c** and **5d**, points to the isopropyloxy group as the preferred phenoxy substituent. The thiophen-2-yl peripheral substituents of compounds **6a–d** induce red-shifted Q-bands to 660–665 nm for compounds **6**, from 635 nm for compounds **5**.

The structure study of **4a** and **4b** shows that the presence of a bulky isopropyloxy ortho-substituent in the phenoxy group in **4b** has induced a small rotation of the thiophene ring from coplanarity with the pyrazine ring as found in **4a**, and a further rotation of the phenoxy ring away from orthogonality compared with the conformation in **4a**. Both changes serve to accommodate the isopropyloxy group which appears to prevent the 180° rotational isomerism of the thiophene ring that was found in **4a**.

5. Supplementary data

CCDC 783407 and 783406 contain the supplementary crystallographic data for (**4a**) and (**4b**). These data can be obtained free of charge via http://www.ccdc.cam.ac.uk/conts/retrieving.html, or from the Cambridge Crystallographic Data Centre, 12 Union Road, Cambridge CB2 1EZ, UK; fax: (+44) 1223 336 033; or e-mail: deposit@ccdc.cam.ac.uk.

Acknowledgement

Mr. Lars Hagen is thanked for technical assistance with the MALDI-TOF analyses.

References

[1] C.C. Leznoff, A.B.P. Lever, Phthalocyanines Properties and Applications, vols. 1–4, VCH, Weinheim, 1989.
[2] (a) S.V. Kudrevich, J.E. Van Lier, Coord. Chem. Rev. 156 (1996) 163;
(b) R. Faust, Eur. J. Org. Chem. (2001) 2797;
(c) F. Mitzel, F. FitzGerald, A. Beeby, R. Faust, Eur. J. Org. Chem. (2004) 1136;
(d) B.H. Lee, J.Y. Jaung, Dyes Pigment 65 (2005) 159;
(e) P. Zimcik, M. Miletin, Z. Musil, K. Kopecky, L. Kubza, D. Brault, J. Photochem. Photobiol. A 183 (2006) 59;
(f) S. Makhseed, F. Ibrahim, J. Samuel, M. Helliwell, J.E. Warren, C.G. Bezzu, N.B. McKeown, Chem. Eur. J. 14 (2008) 4810.
[3] E.H. Mørkved, L.T. Holmaas, H. Kjøsen, G. Hvistendahl, Acta Chem. Scand. 50 (1996) 1153.
[4] E.H. Mørkved, H. Ossletten, H. Kjøsen, Acta Chem. Scand. 53 (1999) 1117.
[5] (a) D. Wöhrle, M. Eskes, K. Shigehara, A. Yamada, Synthesis (1993) 194;
(b) K.I. Ozoemena, T. Nyokong, Inorg. Chem. Commun. 6 (2003) 1192.
[6] S. Makhseed, F. Ibrahim, C.G. Bezzu, N.B. McKeown, Tetrahedron Lett. 48 (2007) 7358.
[7] S. Makhseed, J. Samuel, F. Ibrahim, Tetrahedron 64 (2008) 8871.
[8] (a) D. Wöhrle, N. Iskandar, G. Grashew, H. Sinn, E.A. Friedrich, W. Maier-Borst, J. Stern, P. Schlag, Photochem. Photobiol. 51 (1990) 351;
(b) U. Michelsen, H. Kliesch, G. Schnurpfeil, A.K. Sobbi, D. Wöhrle, Photochem. Photobiol. 64 (1996) 694.
[9] H. Li, T.J. Jensen, F.R. Fronczek, M.G.H. Vicente, J. Med. Chem. 51 (2008) 502.
[10] E.H. Mørkved, T. Andreassen, P. Bruheim, Polyhedron 28 (2009) 2635.
[11] E.H. Mørkved, N.K. Afseth, P. Zimcik, J. Porphyr. Phthalocya. 11 (2007) 130.
[12] A. Nakamura, T. Ataka, H. Segawa, Y. Takeuchi, T. Takematsu, Agric. Biol. Chem. 47 (1983) 1555.
[13] A. Nakamura, T. Ataka, H. Segawa, Y. Takeuchi, T. Takematsu, Agric. Biol. Chem. 47 (1983) 1561.
[14] R.W.W. Hooft, COLLECT Data Collection Software, Nonius B.V., 1998.
[15] Z. Otwinowski, W. Minor, Methods Enzymol. 276 (1997) 307.
[16] Z. Otwinowski, D. Borek, W. Majewski, W. Minor, Acta Crystallogr. A59 (2003) 228.
[17] (a) G.M. Sheldrick, Acta Crystallogr. A46 (1990) 467;
(b) http://shelx.uni-ac.gwdg.de/SHELX.
[18] G.M. Sheldrick, Acta Crystallogr. A64 (2008) 112.
[19] L.J. Farrugia, J. Appl. Crystallogr. 30 (1997) 565.
[20] E. Prince (Ed.), International Tables for Crystallography, vol. C, Kluwer, Dordrecht, 2004, pp. 799–806 (Chapter 9.5).